Steel fiber-reinforced concrete for precast tunnel lining segments

Fanbing SONG, Ruhr-University Bochum, Germany, Fanbing.Song@rub.de
Rolf BREITENBÜCHER, Ruhr-University Bochum, Germany, Rolf.Breitenbuecher@rub.de

Topic: Planning and Designing Tunnels and Underground Structures

Summary:
Precast tunnel lining segments are often subjected to critical impact and concentrated loads especially during the construction stage. The peripheral regions of segments, such as edges and corners, are usually exposed to significantly higher stresses than the interior. Under such high stress concentrations, concrete damages in the form of cracking and spalling are very likely to occur in these surface-near areas. Compared to conventional rebar reinforcement, owing to the crack-bridging effect and a randomly discrete distribution in the matrix, steel fibers can also be used to strengthen the concrete structure, even in the concrete cover.

Based on this fact, a new design concept to manufacture hybrid segments can be feasible. In this paper, hybrid concrete specimens consisting of steel fiber-reinforced concrete in the surface-near layer and plain concrete in the interior were produced by means of a special concreting technique. To simulate the segments subjected to local forces on a small-scale, a concentrated load was transmitted onto the upper surface of these specimens through a steel block. Parameters governing the load-bearing and fracture behavior of concrete under concentrated load, such as load eccentricity, thickness of fiber reinforcement, casting direction and fiber-cocktail, were investigated. The effects of these variables on the ultimate bearing strength, stress-displacement response, failure mode and crack pattern were analysed and discussed.

Keywords: *steel fiber, concentrated loads, load-bearing behavior, crack pattern, hybrid segment*

1. Introduction

In mechanized shield tunneling, precast tunnel lining segments are assembled by erector under the protection of the TBM tail shield into rings. During the construction stage, segments are often subjected to critical impact and concentrated loads primarily due to e.g. pressing force of the TMB [1, 2], dimensional imperfection of segments [3], assembly inaccuracy [2, 4] and offset of segments [4]. Under such highly concentrated loads, not only compressive stresses but also tensile stresses can be generated beneath the partially loaded area [5-7]. If the splitting tensile stresses (perpendicular to the load) exceed the concrete tensile strength, cracking and spalling of concrete occur unavoidably. This phenomenon is more pronounced in the case of high-strength concrete as used for precast segmental linings, where the compressive strength typically ranges from 70 to 90 MPa.

In practice, concrete members under concentrated loads are normally reinforced with transverse rebar reinforcement to withstand the splitting tensile stresses. However, due to adherence to a minimum thickness of the concrete cover, concrete in the near-surface regions can hardly be strengthened. An alternative approach is to add steel fibers into the concrete mixture. Owing to the crack-bridging effect and a randomly discrete distribution of fibers in the matrix, structural members can be effectively strengthened even in the concrete cover. In the last two decades, steel fiber reinforcement has been frequently applied for precast segmental tunnel linings worldwide [8-12].

Based on the fact that the peripheral regions of segments such as corners and edges are usually the most vulnerable areas, and they are subjected to significantly higher stresses than the interior. Instead of a full-scale fiber reinforcement in the entire cross-section of segments, a new design concept to manufacture hybrid segments can be considered, which is characterized by placing steel fiber-reinforced concrete (SFRC) with high-performance in the peripheral regions combined

with normal ferro-concrete or plain concrete (PC) in the interior. Besides potential economical advantages, the engineering properties of the different concretes can be effectively utilized, however, extensive investigations on concrete composite optimization, production techniques and structural behaviour of hybrid segment are required.

In this paper, the experimental program was designed firstly to develop a practicable concreting technique to manufacture small-scaled hybrid concrete elements containing SFRC and PC under laboratory conditions and secondly to investigate the load-bearing and fracture behaviour of these hybrid specimens under concentrated load as a simulation of precast tunnel lining segments subjected to local forces in small-scale. The experimental investigation conducted here serves as a fundamental study on the development of design concept and production techniques of hybrid segmental linings within the scope of a research project "SFB 837 B1: Optimized Hybrid Segments for Durable and Robust Tunnel Lining Systems".

2. Experiments

The principal variables controlling the load-bearing and fracture behavior of concrete under concentrated load, such as thickness of fiber reinforcement, fiber-cocktail, casting direction (or fiber orientation) and load eccentricity, were investigated.

2.1 Materials, specimens and research scope

An ordinary Portland cement CEM I 52.5 R (DIN EN 197-1) was used in this study. The aggregates used consisted of Rhine river sand and gravel with a maximum grain size of 16 mm (grading curve A/B 16, DIN 1045-2). For the production of SFRCs, a base concrete mixture corresponding to a typical concrete composition for precast tunnel lining segments was used throughout the experiment (Table 1). To maintain a proper workability, all SFRCs were modified by adding a higher dosage of a PCE-based superplasticizer.

Two types of steel fiber were applied here: The L fiber (RC-80/60-BN) is a hook-ended macro-fiber; the S fiber (FM 13/0.19) is a straight micro-fiber. The detailed information of the fibers is given in Table 2. The fiber dosage for SFRC with one single fiber type L was 60 kg/m³ (L60) and 120 kg/m³ for SFRC with fiber-cocktail (L60S60, 50 % of L fiber plus 50 % of S fiber).

Table 1 *Proportions of the base plain concrete (PC)*

Cement [kg/m³]	Fly ash [kg/m³]	Aggregate [kg/m³]	Water [kg/m³]	w/c-ratio	Superplasticizer [kg/m³]
330	90	1849	148.5	0.45	1.3

Table 2 *Types and properties of the steel fibers*

Fiber code	Fiber type	Shape	Length [mm]	Diameter [mm]	Aspect ratio [l/d]	Tensile strength [MPa]
L	RC-80/60-BN	hook-ended	60	0.75	80	1225
S	FM 13/0.19	straight	13	0.19	68	2000

For the SFRCs and PC, the compressive strength was determined on 150 mm cubes and the splitting tensile strength and Young's modulus were determined on 150 mm x 300 mm cylinders. All specimens were cast according to DIN EN 12390-2: 2009. The samples were cured in accordance with DIN EN 12390-2: 24h in the molds, 6 days in a water curing tank at 20 ± 2 °C, 21 days in the air at 20 ± 2 °C with RH = 65 ± 5 % (with the exception of the cylinders for the determination of splitting tensile strength, which were further stored in a water tank for 27 days after demolding).

The properties of the fresh as well as hardened PC and SFRCs were determined in accordance with DIN EN 12350, DIN EN 12390 and DIN 1048, as presented in Table 3. All tests were carried out on the concrete samples at an age of 28 days.

Table 3 *Properties of the fresh and hardened PC and SFRCs*

Properties	PC	L60	L60S60
Flow consistency [cm] (DIN EN 12350-5)	42	43	37
Air void content [%] (DIN EN 12350-7)	3.0	1.9	1.3
Bulk density [kg/m³] (DIN EN 12350-6)	2356	2437	2468
Compressive strength [MPa] (DIN EN 12390-3)	84.5	87.4	94.4
Splitting tensile strength [MPa] (DIN EN 12390-6)	4.0	6.7	7.5
Young's modulus [GPa] (DIN 1048-5)	36	37	-

Concrete prisms (150 mm x 150 mm x 300 mm) for the concentrated loading tests were produced in either standing (s) or lying (l) wooden molds. For the production of hybrid concrete (HC) specimens in standing molds, PC was at first filled and compacted to a certain predefined height following the placing of SFRC. For specimen production in a lying form, PC and SFRC were simultaneously placed in the form and temporarily separated by a stainless steel plate with a predefined distance to the internal wall of the mold. During the concreting, the steel plate was successively being lifted up and a monolithic combination of the two concretes in the fresh state was achieved by means of vibration (Fig. 1). The thicknesses of fiber reinforcement are 50 mm, 100 mm and 150 mm, respectively. To prevent any stress concentration through surface roughness, the casting or testing surface (150 mm x 150 mm) of the prisms was plane parallel ground a few days prior to testing. The concentrated loading tests were performed on the concrete prisms at an age of 28 days.

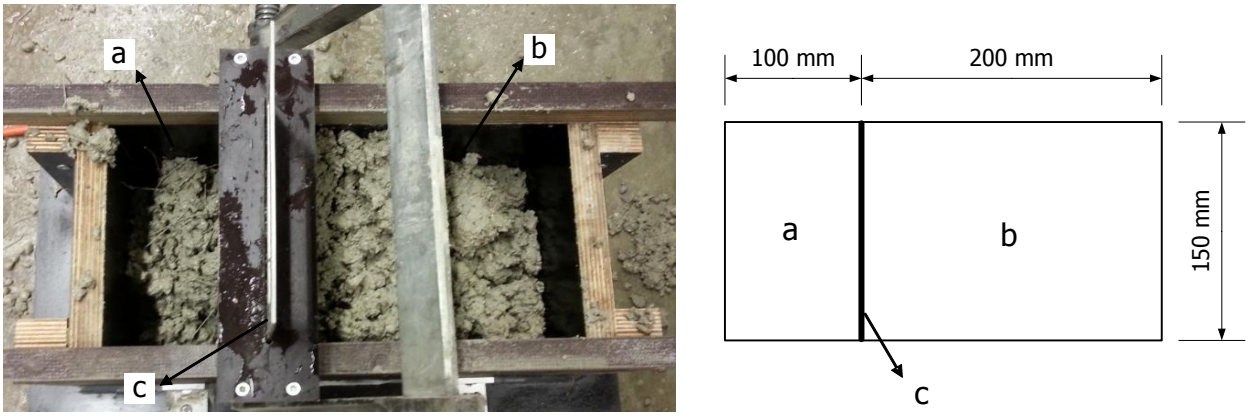

Fig. 1 *Special formwork for the production of hybrid concrete specimen: a) steel fiber-reinforced concrete (SFRC); b) plain concrete (PC); c) temporary partition steel plate*

The test program for specimens produced with L60 fiber reinforcement is listed in Table 4, which is identical with that for specimens reinforced by L60S60 fiber reinforcement. Each testing series consists of 3-4 prisms. All specimens were loaded by a steel plate with a cross-section of 50 mm x 50 mm corresponding to an area ratio of 9 (area ratio: ratio of total area A_c to loaded area A_{c0}). In addition to centric load introduction (m), the specimens were also loaded eccentrically: on the edge (e) or on one corner (c), as illustrated in Fig. 2, right. As a comparison, specimens of PC were tested under the same testing conditions as well.

Table 4 *Test program for specimens produced with L60 fiber reinforcement (FR)*

FR-Type	Mold type	Load introduction	FR-thickness [mm]	Series index
L60	s	m	50	L60_s_m_50
			100	L60_s_m_100
			150	L60_s_m_150
			300	L60_s_m_300
		e	100	L60_s_e_100
			300	L60_s_e_300
		c	100	L60_s_c_100
			300	L60_s_c_300
	l	m	50	L60_l_m_50
			100	L60_l_m_100
			150	L60_l_m_150
			300	L60_l_m_300

2.2 Test set-up and testing procedure

All tests were performed by using a servo-hydraulic universal testing machine with a maximum load capacity of 5 MN. The load was transmitted onto the upper surface of the prism through a steel plate. By use of LVDTs (HBM 1-WA/20MM-T) the horizontal and vertical deformations of the specimen were measured (Fig. 2, left). The load was continuously applied at a loading rate of 0.5 mm/min. The testing process was automatically terminated by the software under the condition that a load drop by 60% of the maximum load was detected. In the case of eccentric (edge and corner) loading, to avoid an overturning of the prism, the specimen was accordingly placed eccentrically on the lower machine platen (Fig. 2, right).

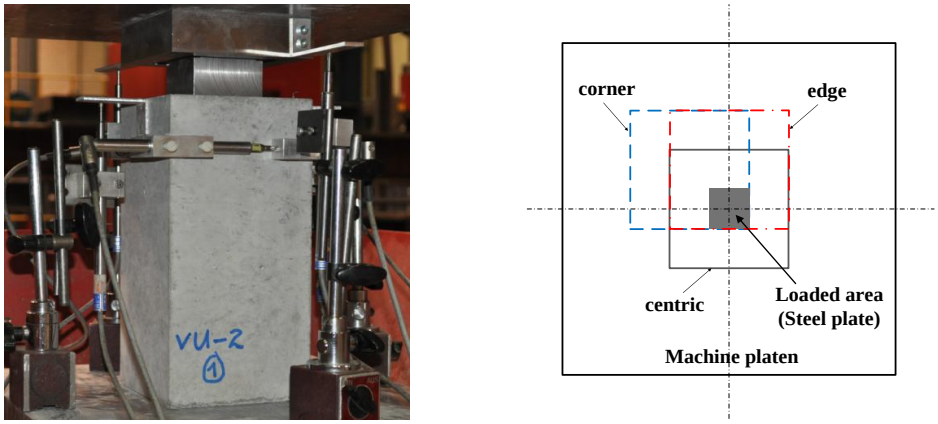

Fig. 2 *Test set-up for concentrated loading tests (left) and positioning of the specimen for centric and eccentric loading (right)*

3. Results

3.1 Ultimate local compressive stress

The mean values of ultimate local compressive stress (σ_{max}, defined as the ultimate force divided by A_{c0}) under centric and eccentric loading are summarized in Tables 5 and 6. For HC samples cast in standing molds under centric loading, a considerable increase in σ_{max} with increasing thickness of fiber reinforcement was observed compared to PC specimens, in particular for fiber-cocktail reinforcement. In this case, by incorporating an only 50 mm thick reinforcement layer (1/6 of the total specimen height), an increase of 30.1 % in σ_{max} was recorded implying a higher effectiveness in improving the bearing capacity. With a 150 mm thick layer of fiber reinforcement (1/2 of the specimen height), all HC samples exhibited the same, or slightly higher values of σ_{max} than those

of SFRC specimens (L60_s_m_150 vs. L60_s_m_300). This indicates that concerning the ultimate load-bearing capacity, a fiber incorporation into the entire specimen is not necessary.

For HC specimens produced in lying molds, the increase in σ_{max} through fiber reinforcement was comparatively unnoticeable, especially for reinforcement layers over 100 mm due to a preferred fiber orientation with respect to the load direction as reported in [13]. As is well known, fibers aligned to the acting direction of tensile stresses (perpendicular to load) have the best crack-bridging capacity. Placing fibers into a thin layer with 50 mm in thickness did not seem to effectively and positively affect the fiber orientation for the cases studied here.

Table 5 *Results of centric concentrated loading tests*

Series index	σ_{max} [MPa]	Δ [MPa]	Δ [%]
PC_m	152	-	-
L60_s_m_50	157	4,9	3,2
L60_s_m_100	194	42,6	28,1
L60_s_m_150	215	63,3	41,7
L60_s_m_300	214	62,8	41,4
L60_l_m_50	160	8,7	5,7
L60_l_m_100	165	13,6	8,9
L60_l_m_150	168	16,1	10,6
L60_l_m_300	173	21,3	14,0
L60S60_s_m_50	197	45,7	30,1
L60S60_s_m_100	247	95,3	62,8
L60S60_s_m_150	270	118,0	77,8
L60S60_s_m_300	266	114,5	75,5
L60S60_l_m_50	158	6,8	4,5
L60S60_l_m_100	181	29,4	19,4
L60S60_l_m_150	188	35,9	23,7
L60S60_l_m_300	201	49,3	32,5

Generally, specimens loaded eccentrically showed lower values of σ_{max} than specimens loaded centrically due to an excessive reduction in confinement effect of the surrounding concrete [14-15]. The bearing strength of HC specimens was also consistent with this tendency. For HC samples with a 100 mm reinforcement layer, the value of σ_{max} was up to 32.5 % higher than that of PC specimens (L60S60_s_c_100 vs. PC_c). Compared to SFRC samples, a maximum reduction in σ_{max} was only 11.8 % (L60S60_s_e_100 vs. L60S60_s_e_300). Notice that, HC specimens with a fiber-cocktail had the same bearing strength as that of SFRC samples under corner loading.

Table 6 *Results of eccentric concentrated loading tests*

Series index	σ_{max} [MPa]	Δ [MPa]	Δ [%]
PC_e	113	-	-
PC_c	83	-	-
L60_s_e_100	129	16	14,2
L60_s_e_300	141	28	24,8
L60_s_c_100	100	17	20,5
L60_s_c_300	110	27	32,5
L60S60_s_e_100	142	29	25,7
L60S60_s_e_300	161	48	42,5
L60S60_s_c_100	110	27	32,5
L60S60_s_c_300	110	27	32,5

3.2 Stress-displacement behavior

Figures 3-5 show the influences of the investigated variables on the stress-longitudinal displacement response of PC, HC and SFRC specimens under centric or eccentric loading, respectively. It can be seen that under a given testing condition the structural stiffness for all concrete specimens is nearly identical in the pre-peak branch. In the case of specimen production in standing molds, the casting direction is identical to the loading direction. With increasing reinforcement thickness, HC specimens exhibited not only an increase in load-bearing capacity but also a remarkable improvement in post-cracking ductility in comparison to PC samples. For a reinforcement thickness of 150 mm, besides an almost identical σ_{max}, HC prisms with L60 reinforcement showed nearly the same ductile post-cracking behavior as that of SFRC prisms (Fig. 3, left). However, for L60S60 reinforcement, SFRC specimens exhibited a quite more ductile behaviour even with a slightly lower σ_{max} (Fig. 3, right). It can be explained as following: With the proceeding of crack propagation, fibers in the lower section of specimen were also activated and the crack-bridging effect was further enhanced by the synergy of the fiber-cocktail.

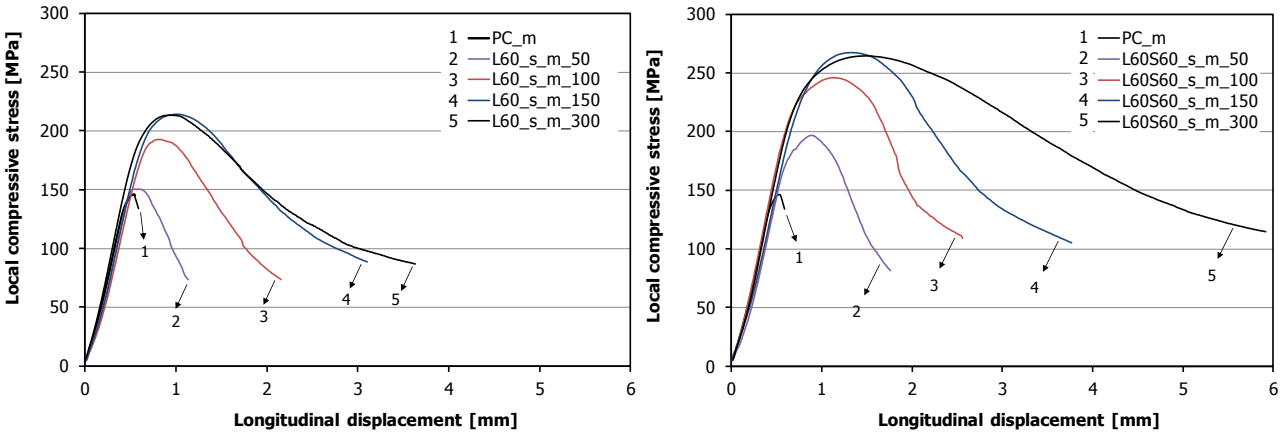

Fig. 3 *Stress displacement response of concrete specimens cast in standing molds under centric loading: left for L60 reinforcement and right for L60S60 reinforcement*

For concreting in lying molds, despite an unremarkable increase in σ_{max} in comparison with PC, HCs with L60 reinforcement exhibited a certain improvement in the ductility (Fig. 4, left). Nevertheless, no noticeable difference in the post-cracking behavior was found for reinforcement thicknesses over 100 mm. For HCs with L60S60 reinforcement, although the increase in σ_{max} and material ductility was slightly higher, compared to HCs cast in standing molds, this improvement was even not comparable. In other words, the casting direction (fiber orientation) exerts more dominant influence on the load bearing behavior of concrete reinforced by steel fibers than the type or thickness of fiber reinforcement does.

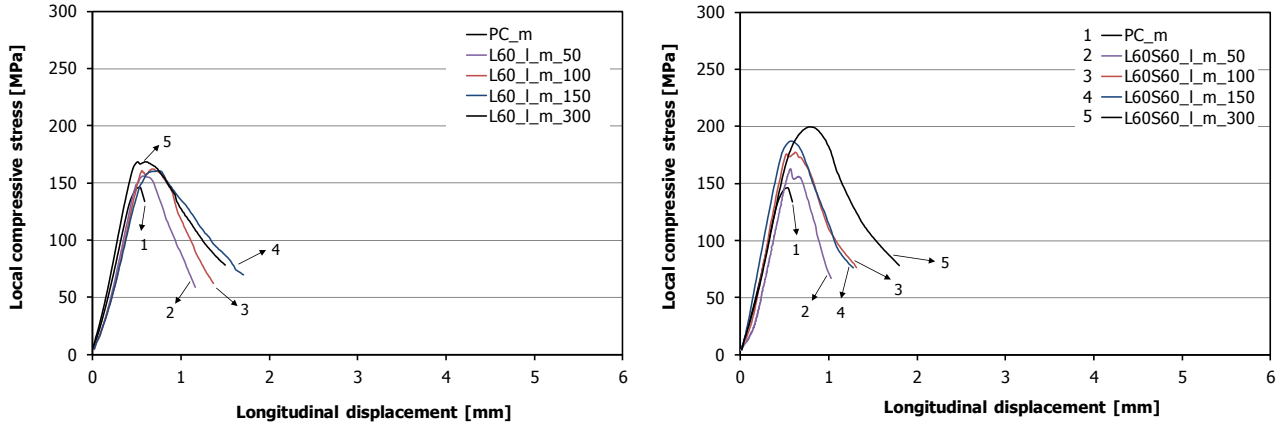

Fig. 4 *Stress displacement response of concrete specimens cast in lying molds under centric loading: left for L60 reinforcement and right for L60S60 reinforcement*

In the case of eccentric loading, by incorporating 100 mm thick fiber reinforcement, a ductile post-cracking behavior can be introduced to the concrete, as shown Fig. 5. The ductile behavior of SFRC specimens with L60S60 reinforcement, as explained above, is related to the activation of fibers in the lower section and a synergy effect in crack-bridging of the fiber-cocktail.

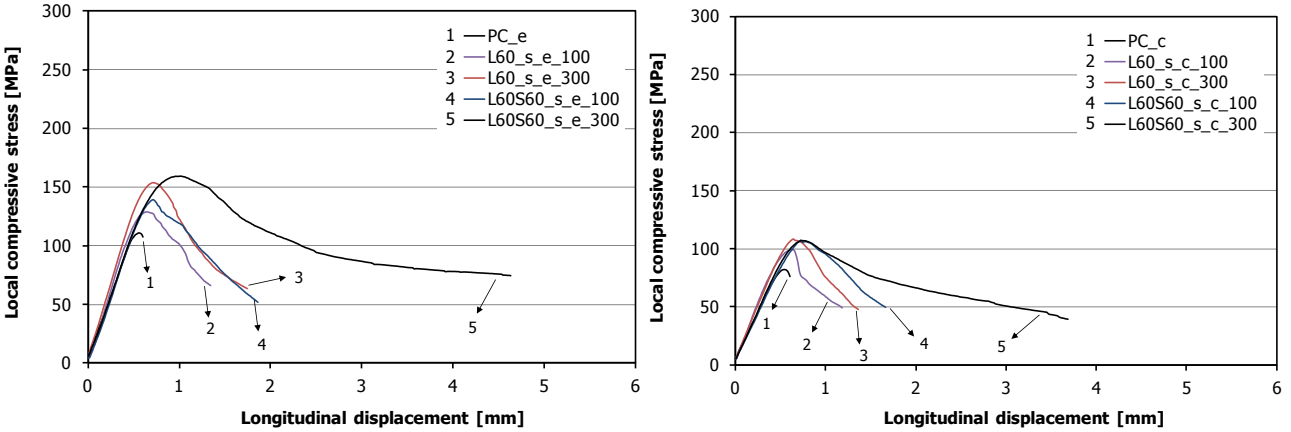

Fig. 5 *Stress displacement response of concrete specimens cast in standing molds under eccentric loading: left for L60 reinforcement and right for L60S60 reinforcement*

3.3 Failure mode and crack pattern

For all concrete specimens, no visible cracking or spalling was observed until shortly before reaching the ultimate load. Soon afterwards, all PC specimens showed a brittle failure, especially under edge loading (Fig. 7e). Specimens produced with fiber reinforcement, even in the case of HC samples only with 50 mm thick reinforcement, showed a ductile fracture behavior.

Under centric loading, HC prisms cast in standing molds shared a similar crack pattern with that of SFRC samples, which is characterized by a random multi-crack distribution on the testing surface and longitudinal crack propagation on the lateral surfaces (Fig. 6c). However, for HC specimens, the cracks on the lateral surfaces spread over half of the height of the specimens (Fig. 6b). This typical crack pattern of HC specimens is independent of the thickness or type of fiber reinforcement. For HC specimens reinforced by L60S60 reinforcement, in addition to longitudinal cracks, transverse cracks were also observed propagating along the borderline of the PC and SFRC layer on the lateral surfaces.

For concreting in lying moulds, the crack pattern of HC and SFRC specimens under centric load is almost identical and characterized by two main cracks starting from the testing surface and propagating through the lateral surfaces (parallel to yz cross-section [16]) and independent of the thickness or type of fiber reinforcement, as demonstrated in Fig. 6 d-f.

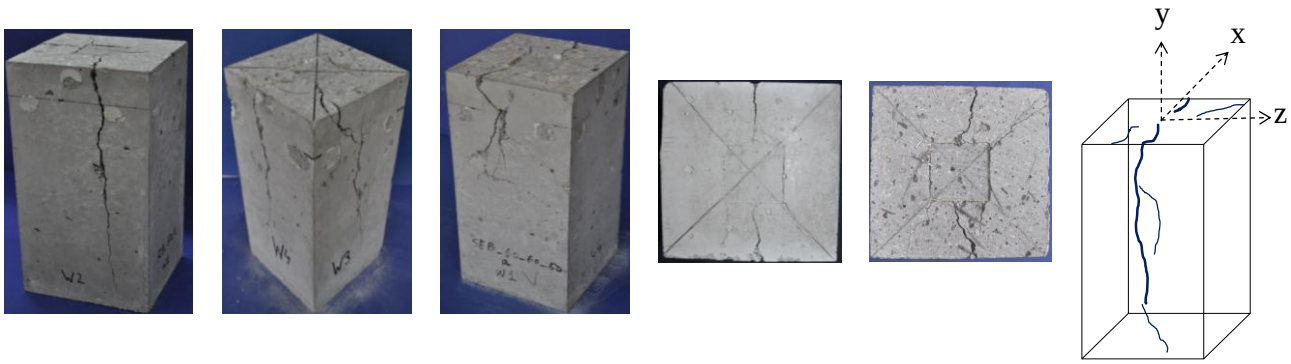

a) PC_m *b) L60_s_m_150* *c) L60_s_m_300* *d) L60_s_l_50* *e) L60_s_l_300* *f) crack distribution*

Fig. 6 *Typical examples of tested specimens produced in standing molds under centric loading*

In the case of corner loading, HC samples reinforced by 100 mm fiber reinforcement showed a nearly identical failure pattern to that of SFRC specimens. No fatal concrete damages were found even by PC samples under defined testing conditions. On the contrary, under edge loading, for PC samples concrete adjacent to the loaded area was one-sidedly punched out (Fig. 7d). The HC specimens remained their integrity after the test, however, two main diagonal continuous cracks were observed on the lateral surface in addition with minor concrete spalling close to the specimen bottom (Fig. 7e), whereas the concrete damages of SFRC specimens were restricted to local regions under the loaded area (Fig. 7f).

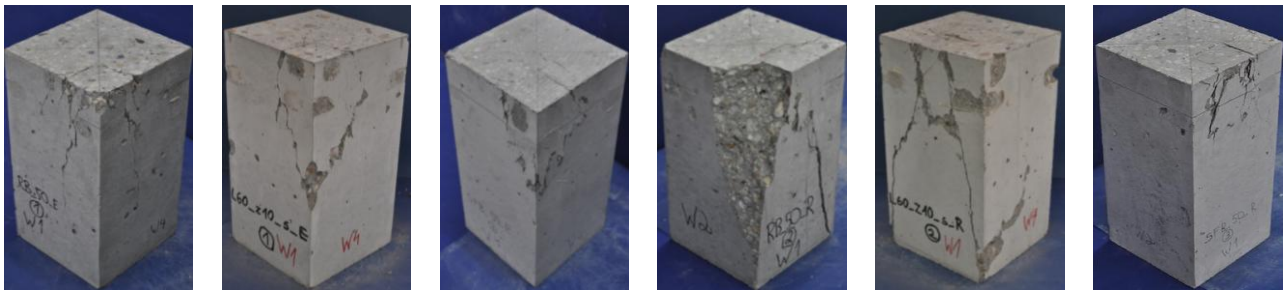

a) PC_c *b) L60_s_c_100* *c) L60_s_c_300* *d) PC_e* *e) L60_s_e_100* *f) L60_s_e_300*

Fig. 7 *Typical examples of tested specimens produced in standing molds under eccentric loading*

4. Conclusions and Discussions

A series of concentrated loading tests on plain concrete, hybrid concrete and steel fiber-reinforced concrete prisms was carried out. The influences of thickness of fiber reinforcement, fiber-cocktail, casting direction (or fiber orientation) and load eccentricity were systematically investigated.

Incorporating a thin layer of steel fiber reinforcement into plain concrete led to a considerable increase in the load-bearing capacity and changed the failure mode of concrete from a brittle to a ductile one, not only for centric but also for eccentric loading situations. This positive effect can be further enhanced by increasing the thickness of fiber reinforcement or using a fiber-cocktail. Therefore, it is highly recommended to use hybrid steel fiber-reinforced high-performance concrete to strengthen the surface-near regions of the segments. However, the mixture composition and properties of this fiber concrete in fresh and hardened states should be intensively investigated as well as its compatibility with the concrete in the interior.

Varying the casting direction exerted a preferred fiber orientation in the concrete, even in a thin layer; compared with other factors, fiber orientation had a more dominant effect on the load-bearing behavior of concrete under concentrated loads. Thus, a preferred fiber orientation perpendicular to the load direction is essential to ensure a higher bearing capacity and a better crack resistance. To achieve this, further experiments should be performed with the focus on the interaction among fiber reinforcement thickness and properties of SFRC (concrete consistency, fiber types and dosages etc.) and production techniques (concreting direction etc.).

Concrete under eccentric loading, particularly in the case of edge loading, was more vulnerable to concentrated load than concrete under centric loading. Based on this, a multi-lateral fiber reinforcement in the near-surface regions of the specimen should be taken into account. In the case of segmental tunnel linings, all the external sides of segment (contacting with soils and adjacent segments) should be strengthened by fiber reinforcement to effectively withstand the directionally unpredictable impact loads or concentrated loads.

Acknowledgement

Financial support was provided by the German Science Foundation (DFG) in the framework of project "Optimized Structural Segments for Durable and Robust Runnel Lining Systems" of the Collaborative Research Center SFB 837. This support is gratefully acknowledged.

References

[1] Grübl, F.: Einschaliger Tunnelausbau mit Stahlbetontübbingen – Welche Lasten sind maßgebend, wie kann man Schäden vermeiden? Tunnelbau 1998, German Geotechnical Society, pp.323–347.

[2] Winselmann, D.; Städing, A.; Babendererde, L. ; Holzhäuser, J.: Aktuelle Berechnungsmethoden für Tunnelauskleidungen mit Tübbingen und deren verfahrenstechnische Voraussetzungen. DGGT 2000 – Baugrundtagung, Hannover, 2000.

[3] Baumann, T.: Tunnelauskleidung mit Stahlbetontübbingen. Bautechnik 69, pp. 11-20, 1992.

[4] Balthaus, H.; Dorgarten, H.-W.; Billig, B.: Tunnelsicherung und –ausbau. Beton-Kalender 2005, pp.257–381.

[5] Heilmann, H.G.: Versuche zur Teilflächenbelastung von Leichtbeton für tragende Konstruktionen. Deutscher Ausschuss für Stahlbeton, Heft 344, 1983.

[6] Leonhardt, F.: Vorlesung über Massivbau, Teil 2. Sonderfälle der Bemessung im Stahlbetonbau. Springer-Verlag, Berlin, 3. Auflage, 1986.

[7] Breen, J. E. et al.: Anchorage Zone Reinforcement for Post-Tensioned Concrete Girders, National Cooperative Highway Research Program, Report 356, 1994.

[8] Moyson, D.: The construction of a steel fibre reinforced concrete segmental lining in London. In: Weltneuheiten im Tunnelbau, Proceedings of the World Tunnel Congress/STUVA-Tagung'95 Stuttgart, Germany. Alba, Düsseldorf, pp. 274–278, 1995.

[9] Kooiman, A.G.; van der Veen, C.; Djorai, M.H.: Steel fibre reinforced concrete segments in the second Heinenoord tunnel. fib Symposium Prague, Czech Republic, Oct. 1999, pp. 13–15.

[10] Woods, E.; Battye, G.: Design decisions for CTRL 2's bored tunnels. Tunnels and Tunnelling International 35 (9), Supplement CTRL Section 2 Tunnelling, pp. 8–10, 2003.

[11] Kasper, K.; Edvardsen, C.; Wittneben, G.; Neumann, D.: Lining design for the district heating tunnel in Copenhagen with steel fibre reinforced concrete segments. Tunnelling and Underground Space Technology 23 (2007), pp. 574-587.

[12] Winterberg, R.; Vollmann, G.: Einsatz von Stahlfaserbeton in der Tübbingproduktion. Tunneling, BFT 04/2009, pp. 4-15.

[13] Breitenbücher, R.; Meschke, G.; Song, F.; Hofmann, M.; Zhan, Y.: Experimental and numerical study on the load-bearing behavior of steel fiber reinforced concrete for precast tunnel lining segments under concentrated loads. In Proceedings of FRC 2014 Joint ACI-fib International Workshop: Fibre Reinforced Concrete: from Design to Structural Applications, 24-25 July 2014, Montreal, Canada, pp. 431-443.

[14] Hawkins, N. M.: The bearing strength of concrete loaded through rigid plates. Magazine of Concrete Research, Vol. 20, No.62, pp. 31 – 40, 1968.

[15] Niyogi, S. K.: Bearing strength of concrete - geometric variations. Journal of the structural division, pp. 1471-1490, 1973.

[16] Breitenbücher, R.; Song, F.: Verhalten von Stahlfaserbeton unter Teilflächenbelastung. Festschrift zum 60. Geburtstag von Josef Hegger: Massivbau im Wandel, Verlag Ernst & Sohn, S. 207-217, 2014.